Revista Mexicana de Astronomía y Astrofísica, **41**, 443–451 (2005)

NUMERICAL SIMULATIONS OF THE FRAGMENTATION OF PHOTOEVAPORATING NONUNIFORM CLUMPS

R. F. González,[1,2] A. C. Raga,[1] and W. Steffen[3]

Received 2005 April 22; accepted 2005 May 25

RESUMEN

En este trabajo, presentamos simulaciones hidrodinámicas en tres dimensiones de la interacción de núcleos neutros inhomogéneos con un flujo externo de fotones ionizantes (plano-paralelo). Mostramos que, como una consecuencia de la estratificación inicial de densidad que supusimos para el núcleo neutro, se producen múltiples condensaciones conforme el núcleo es fotoevaporado. Mostramos también que, en los modelos donde los picos y valles de la variación en densidad están alineados con el flujo de fotones, la fragmentación es más importante y, con una longitud de onda y amplitud de la variación en densidad adecuadas, los fotones ionizantes pueden producir huecos en el núcleo neutro antes de que sea completamente fotoevaporado. Sin embargo, no obtenemos una división del núcleo neutro original en núcleos más pequeños.

ABSTRACT

In this paper, we present 3D gasdynamical simulations of the interaction of nonuniform clumps with an external (plane-parallel) ionizing photon flux. We show that, as a consequence of the initial density stratification that we assumed for the clump, multiple condensations are produced as the clump is photoevaporated. We also show that, in models where the peaks and valleys of the density variability are aligned with the photon flux, this fragmentation is more important and, with an adequate amplitude and wavelength of the density variability, the ionizing photons can produce hollows in the clump before it is completely photoevaporated. However, we do not obtain a division of the original clump into smaller clumps.

Key Words: **ISM: H II REGIONS — ISM: KINEMATICS AND DYNAMICS — ISM: PLANETARY NEBULAE**

1. INTRODUCTION

The interaction of a neutral clump with an external ionizing photon flux has been studied in the past by several authors.

Dyson (1968) modeled a spherical, self-gravitating, neutral condensation immersed in an H II region. He described its evolution due to the gas expelled by ionization from the surface of the neutral condensation (photoevaporating flow).

Bertoldi (1989) and Bertoldi & McKee (1990) developed an approximate analytic model for the evolution of an interstellar cloud which is exposed to the ionizing radiation of a newly formed star. Bertoldi (1989) derived the structure of a steady, photoevaporating, gas flow and he showed that the ionization front moving into the neutral gas is approximately D-critical (as was assumed by Dyson 1968) and that the ionized gas expands supersonically into the intercloud medium. Bertoldi & McKee (1990) studied the evolution of a photoevaporating cloud beyond its initial radiation-driven implosion, showing that the imploded cloud attains a steady, cometary shaped configuration in which the post-ionization front pressure balances the pressure of the neutral gas. They also found that the velocity of the cloud due to the rocket effect of the evaporating gas (Oort & Spitzer 1955) can have values from ~ 5 km s^{-1} for thermal clouds to ~ 10 km s^{-1} for magnetic clouds.

[1]Instituto de Ciencias Nucleares, Universidad Nacional Autónoma de México, México, D. F., México.

[2]Present address: Centro de Radioastronomía y Astrofísica, Universidad Nacional Autónoma de México, Morelia, Mich., México.

[3]Instituto de Astronomía, Universidad Nacional Autónoma de México, Ensenada, B. C., México.

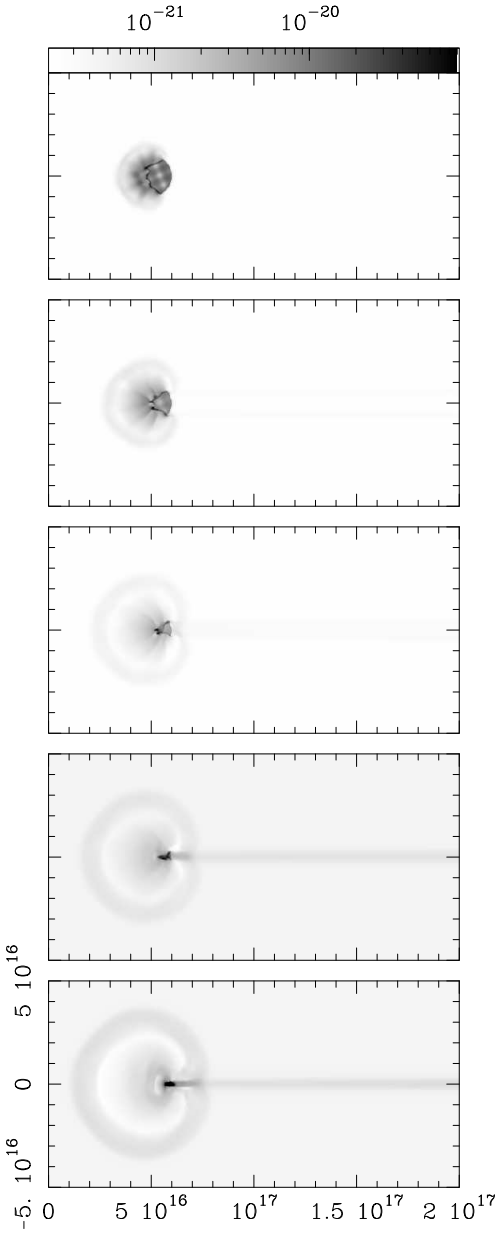

Fig. 1. Time-sequence log-scale maps of the density stratification (given in g cm^{-3} by the bar on the top) on the xz-plane for model M1. The five frames correspond to the integration times from 100 yr (top frame) to 500 yr (bottom frame) in intervals of 100 yr. The x and z axes are labeled in cm.

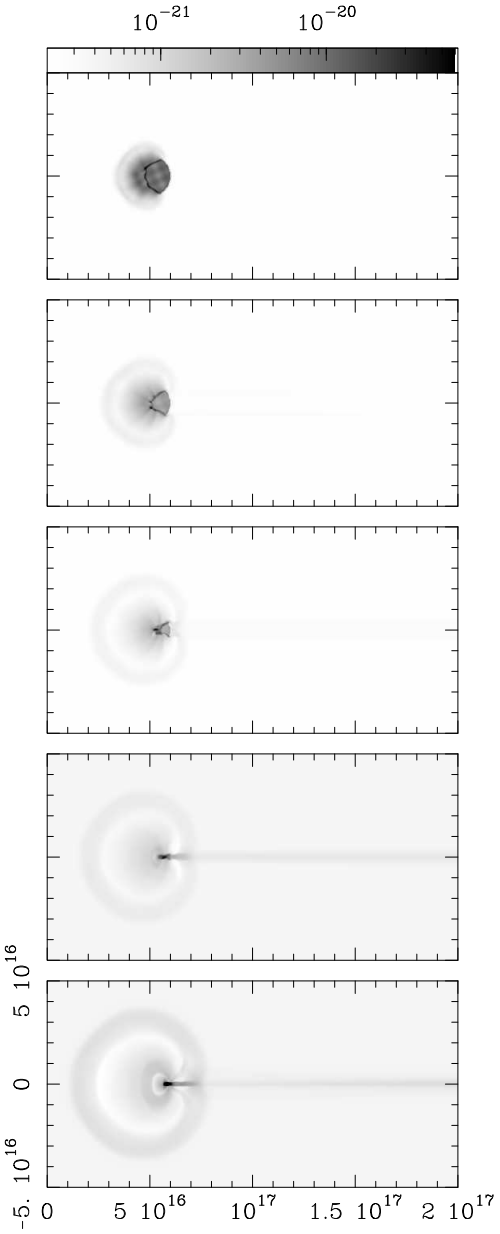

Fig. 2. The same as Fig. 1, but for model M2.

Pastor, Cantó, & Rodríguez (1991) modeled the radio continuum emission from partially ionized globules. Taking into account the acceleration of the outflowing ionized gas, they showed that a characteristic spectrum is formed depending only on the expansion velocity law of the outflowing ionized gas. Their model results fit well the observed radio emission from partially ionized globules in the Orion nebula.

Numerical models of photoevaporated flows have also been calculated. Lefloch & Lazareff (1994) carried out 2D hydrodynamical simulations of the evolution of the cometary globules (which consist of a dense core prolonged by a long tail and surrounded by a bright rim) commonly found in the vicinity of OB stars in H II regions (e.g., O'Dell, Wen, & Hu 1993; Bally, O'Dell, & McCaughrean 2000). Based on the radiation-driven implosion model proposed by

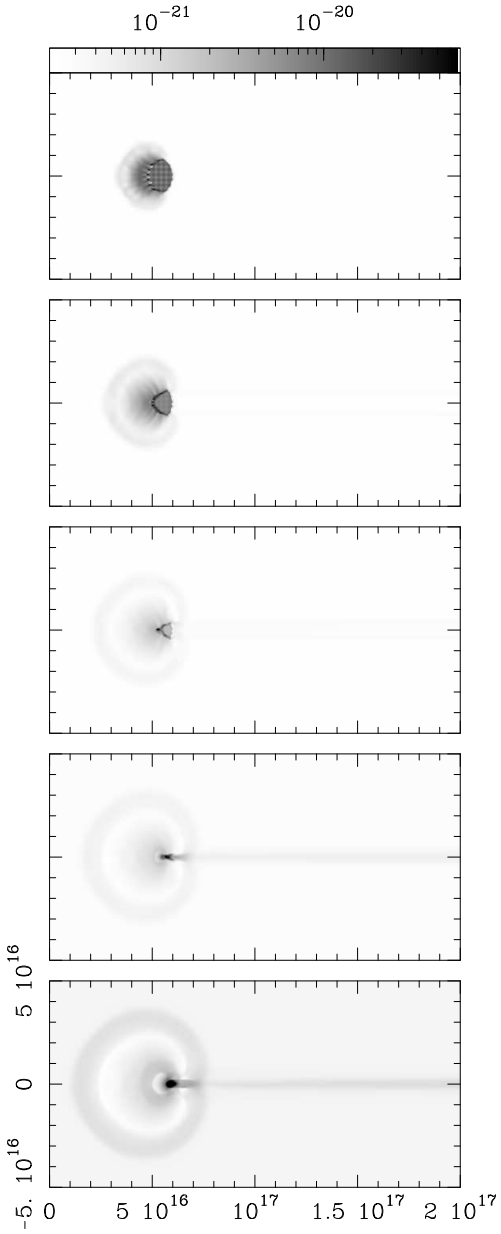

Fig. 3. The same as Fig. 1, but for model M3.

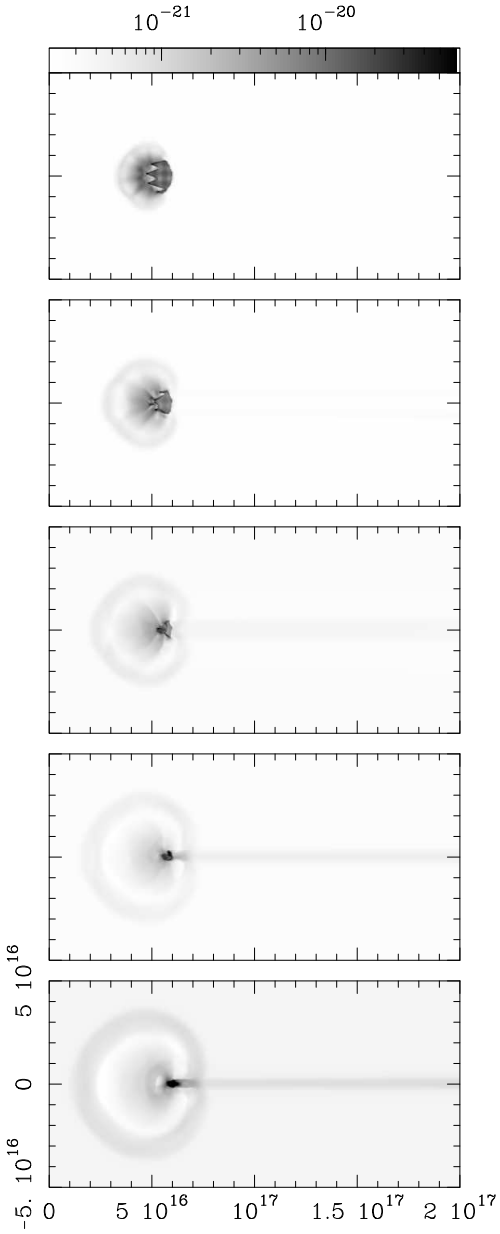

Fig. 4. The same as Fig. 1, but for model M4.

Reipurth (1983), Lefloch & Lazareff (1994) investigated the evolution of cometary globules finding that it is a two-stage process. The collapse phase (which occurs over a short time scale) possibly leading to star formation, and the cometary phase (which lasts approximately 90% of the cloud's lifetime) in which the globule is in a quasi-hydrostatic equilibrium.

The process of photoionization of dense, neutral clumps is also present in the outer parts of planetary nebulae. The evolution of these clumps was studied with both analytic and numerical approaches by Mellema et al. (1998). The radiation from the central star produces a photoevaporating flow and a shock moving through the clump and, once it has run through the entire clump, the clump is accelerated because of the rocket effect (Oort & Spitzer 1955). The analytic and numerical models presented by Mellema et al. (1998) give the velocity, mass and shape of the clump as a function of time, and also reproduce many features of the fast moving low ionization knots observed in planetary nebulae.

Other examples of photoevaporated flows are neutral disks surrounding low-mass, pre-main-sequence stars exposed to an external ionizing pho-

ton field. These objects are called "proplyds" and were described by O'Dell et al.(1993). A few years later, Henney & Arthur (1998) studied the photoevaporated flow from proplyds. Their analytical models can reproduce the observed Hα intensity profiles of the Orion proplyds. Also, they found evidence for freely expanding photoevaporated flows (from the ionization front) with initial Mach numbers close to unity, which are consistent with the theoretical prediction of D-critical ionization fronts.

In some astrophysical sources the interaction of a neutral clump with an impinging external wind+ionization photon flux is present. For instance, this situation is found for clumps embedded within the wind of an O star, and for clumps exposed to the ionizing photon field from the exciting stellar source of an expanding H II region.

This is the case of the proplyds observed in the Orion nebula, which have tails pointing away from θ^1C Ori. Henney et al. (1996) modeled these objects taking into account both the fast wind and the ionizing photon flux of θ^1C Ori. They found two possible solutions to the problem, depending on the value of the ionizing photon flux and the momentum flux of the wind. Strong, ionizing photon fluxes produce photoevaporated flows which interact with the impinging wind forming a detached two-shock structure. For lower ionizing photon fluxes, the wind interacts directly with the surface of the neutral clump and the photoevaporated material is confined to a thin shell surrounding the neutral structure. Henney et al. (1996) argued that models with strong, ionizing photon fluxes can describe the proplyds in the Orion nebula.

In order to study the transition between the "low ionizing photon flux" and the "high ionizing photon flux" regime, Raga, Steffen, & González (2005) investigated through 3D numerical simulations the fragmentation of photoevaporating, nonuniform density clumps (with small amplitude density variabilities) embedded in a stellar wind. In agreement with previous models, we showed that the interaction of a dense clump with an impinging wind leads to the fragmentation of the clump. Also, we showed that the presence of an ionizing photon flux reduces this fragmentation and, for strong enough photon fields, only a single condensation is produced.

Assuming stronger density stratifications, in the present paper we investigate (through 3D gasdynamical simulations) the fragmentation of neutral clumps by the interaction with an impinging ionizing photon flux. This work is an analysis of the importance of the nature of the initial density inhomogeneities for the fragmentation of a photoevaporated clump. The paper is organized as follows. In § 2, we describe the model and present our numerical simulations. A discussion of the results obtained from the simulations is presented in § 3. Finally, in § 4 we give our conclusions.

2. NUMERICAL SIMULATIONS

In this section, we present 3D gasdynamical simulations carried out with the adaptative grid "Yguazú-a" code developed by Raga, Navarro-González, & Villagrán-Muniz (2000). The version of the code that has been used, which is described in detail in Raga & Reipurth (2004), solves the gasdynamic equations, a rate equation for neutral hydrogen, and the radiative transfer of ionizing photons at the Lyman limit. The diffuse radiation is only considered using the case B recombination coefficient.

The calculations were performed on a six-level, binary adaptative grid with a maximum resolution of 3.9×10^{14} cm along the three axes. The computational domain extends over $10^{17}\times10^{17}$ cm in the yz-plane, and 2×10^{17} cm along de x-axis.

2.1. *The Models*

We have computed four different models in order to investigate the interaction of an impinging ionizing photon flux (plane-parallel, directed along the x-axis) with a neutral, nonuniform clump. In all of the runs, we have assumed an isothermal neutral clump with temperature $T_c = 100$ K, radius $r_c = 10^{16}$ cm, and mean density $\overline{n} = 5000$ cm^{-3}. The clump is initially centered in the middle of the yz-plane and is placed at a distance $x_0 = 5\times10^{16}$ cm from the left boundary of the x-axis.

Let A and λ be the amplitude and the characteristic wavelength of the density variability (respectively) of the initial neutral clump. Then, the nonuniform density n_c of the clump is taken to be

$$n_c(x,y,z) = \overline{n}\left[1+\frac{1}{3}A\left(\sin\left[2\pi\frac{x\cos\theta - z\sin\theta}{\lambda}\right]+\right.\right.$$

$$\sin\left[2\pi\frac{-x'\sin\theta + y\cos\theta}{\lambda}\right]+$$

$$\left.\left.\sin\left[2\pi\frac{x\sin\theta + z\cos\theta}{\lambda}\right]\right)\right], \qquad (1)$$

where $x' = x\cos\theta - z\sin\theta$, and θ gives the rotation of the density stratification in the xz and $x'y$-planes.

In Table 1, we list the models that we have considered in this paper. The four models were selected

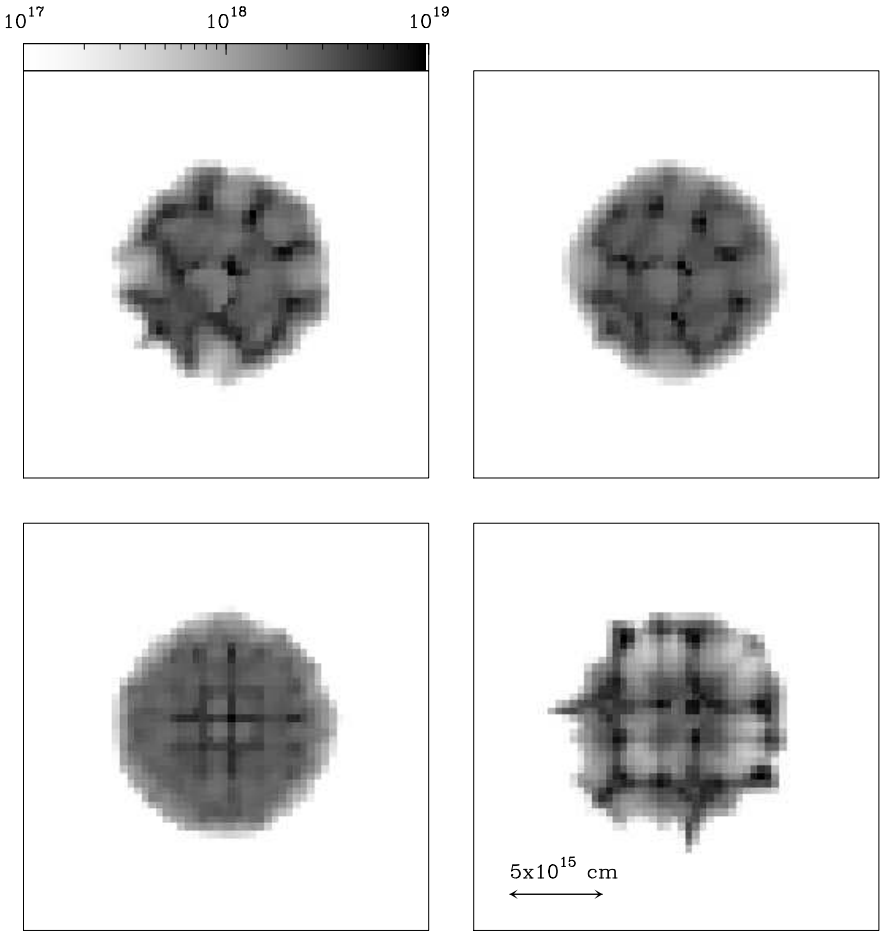

Fig. 5. Column densities (in cm^{-2}) integrated along the x-axis for the 200 yr time frames of models M1 (top left), M2 (top right), M3 (bottom left) and M4 (bottom right). The logarithmic grey scale and the spatial scale of the plots are indicated by the bar at the top left and the arrow at the bottom right, respectively.

with different combinations of the free parameters A, λ and θ. While in models M1 and M2 we changed the amplitude A of the density variability (fixing λ and θ), in models M3 and M4 we varied the wavelength λ (fixing A and θ). In addition, from a comparison between models M1 and M4 we studied the effect of rotating the density stratification (see Eq. [1]). In all models, we assume an impinging ionizing photon flux of 3.98×10^{10} cm^{-2} s^{-1}, which corresponds to a source emitting 5×10^{47} s^{-1} ionizing photons per unit time at a distance of 10^{18} cm.

Figures 1 to 4 show the numerical results obtained from our models M1–M4. Time-sequences (from t = 100 to 500 yr) of the xz-plane density stratifications are depicted for the different models. In all of them, the formation of an irregular ionization front is seen, because regions with different densities at different positions within the clump photoevaporate at different rates. The interaction of the photoevaporated wind with the surrounding medium forms a detached, two-shock structure with very similar and regular shapes in all models. We also observe that the barycenter of the neutral clump material moves along the x-axis to the right of the central position of the initial clump due to the rocket effect. Before every clump is completely photoevaporated, an elongated, high density structure is produced by the high pressure of the photoevaporated material. Besides, some irregular features of photoevaporated material are formed behind the ionization front, before the clump is completely ionized.

At late evolutionary times, our four models produce tail-like neutral structures extending away from the photoionizing source. These tails represent the recombination of the H II region material in the shadow behing the neutral clump. The production of these neutral regions is a direct result of the fact that we do not consider the diffuse, ionizing radiation

(other than by considering the case B recombination coefficient). Cantó et al. (1998) and Pavlakis et al. (2001) have studied these shadow regions with 1D and 2D models (respectively), and have shown that depending on the parameters of the H II region the shadows can be fully photoionized by the diffuse radiation. Therefore, the neutral "shadow structures" obtained in our simulations might actually not be present in many of the observed clumps.

Also, we can observe that multiple structures of neutral material with different densities are formed as the clumps are photoevaporated. For instance, this effect is clearly seen for the 200 and 300 yr evolutionary states presented in Figs. 1–4. Additionally, from the early frames of Figs. 3 and 4, corresponding to models M3 and M4 (in which the peaks and valleys of the density variability are aligned with the impinging plane-parallel ionizing photon flux, i.e., $\theta = 0$), we observe that the ionizing photons penetrate deeper into the neutral clump along the lower density paths (parallel to the x-axis). In particular, the clump in model M4 is completely fragmented after 200 yr of evolution. These results lead us to investigate whether or not an impinging ionizing photon flux is able to produce multiple condensations from a nonuniform clump.

In the following section, we study the clump fragmentation by an impinging ionizing photon flux. We investigate whether the photons are able to divide the clump into smaller structures which are not connected by neutral material with lower densities, i.e., whether or not the ionizing radiation can fragment the original clump into several clumps with smaller physical sizes.

3. CLUMP FRAGMENTATION

In this section, we study the fragmentation of neutral clumps produced by an impinging ionizing photon flux. In Figs. 1–4, we observe (at the earlier times of evolution) that several condensations are produced behind the ionization front, where the neutral material is compressed.

In order to illustrate the condensation structures formed in our models, in Figure 5 we present the column density maps (in the yz-plane) obtained by integrating the number density along the x-axis for the $t = 200$ yr evolutionary states of models M1–M4. Very similar structures result from models M1 and M2 (which differ only in the amplitude of the initial density stratification), in which multiple structures are formed as neutral material is being photoevaporated. Models M3 and M4, in which we have assumed $\theta = 0$ and different wavelengths λ (see Eq. [1]), show very different fragmentation processes. While the clump of model M3 shows the weakest fragmentation of our models, in model M4 the clump is strongly fragmented showing low density paths where the ionizing radiation has penetrated deeper into the neutral material. We also note from a comparison between models M1 and M4, that the variation of the parameter θ leads to very different fragmentation processes of the neutral clump.

In order to quantify the 3D condensation structures produced in models M1–M4, we have analyzed the $t = 200$ yr frames shown in Fig. 5 (see also Figs. 1–4). First, we define a cutoff density n_{cut} (varying from $1{\times}10^4$ cm^{-3} to $1.1{\times}10^5$ cm^{-3} in intervals of $1{\times}10^4$ cm^{-3}), and then we count the number of condensations N_c for each value of n_{cut} (each condensation being defined as a connected volume with

TABLE 1

CLUMP MODELS[a]

Model	A	λ/r_c	θ
M1	0.90	0.50	$\pi/8$
M2	0.50	0.50	$\pi/8$
M3	0.90	0.25	0
M4	0.90	0.50	0

[a]The parameters of models are described in § 2.

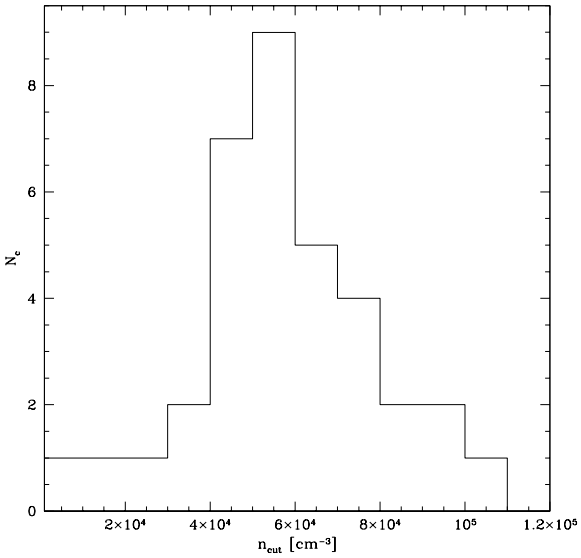

Fig. 6. Number of clumps as a function of the cutoff density obtained from the 200 yr frame of the 3D density map of model M1 (Fig. 1).

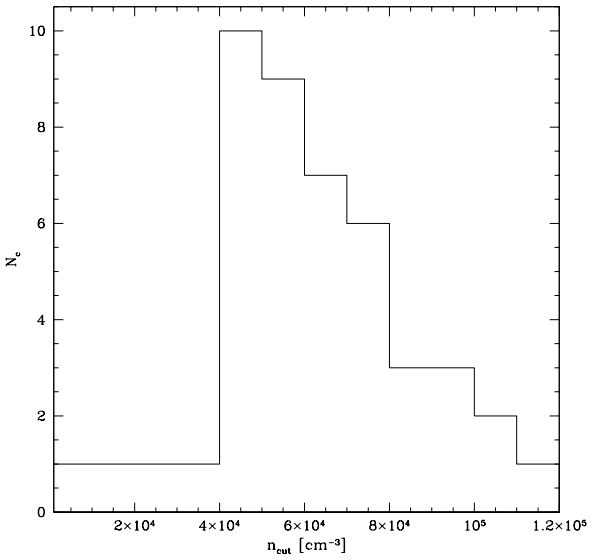

Fig. 7. The same as Fig. 5, but for model M2 (Fig. 2).

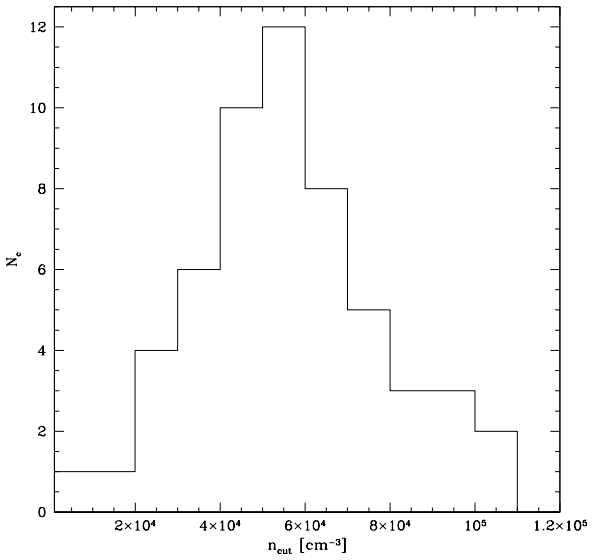

Fig. 9. The same as Fig. 5, but for model M4 (Fig. 4).

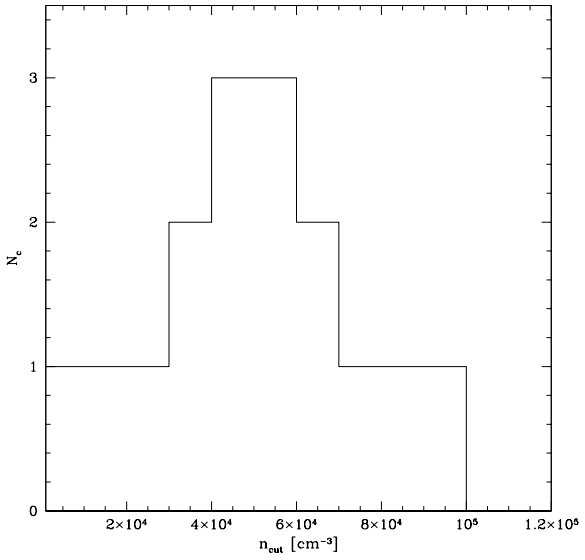

Fig. 8. The same as Fig. 5, but for model M3 (Fig. 3).

density $n > n_{cut}$). In order to count only density structures with relatively high peaks with respect to their surroundings, we have only considered the condensations which satisfy that $n/n_{cut} \geq 2$.

Our results are presented in Figures 6 to 9. In all models it can be observed that, for low enough cutoff densities, the clump is seen as a single condensation ($N_c = 1$). No clumps are detected ($N_c = 0$) for cutoff densities higher than the maximum density found in each simulation. In all models the cutoff densities for non-detection of condensations are much higher than the peak value of the initial density variablity (Eq. [1]), according to the fact that the neutral material is compressed as the clump is photoevaporated.

All graphs show a similar behaviour of N_c versus n_{cut}. For low cutoff densities, we observe an increasing number of condensations as the cutoff densities increase. After the maximum number of condensations $N_c(max)$ is reached, N_c begins to decrease for higher n_{cut} densities. We see that $N_c(max)$ and the value of n_{cut} at which the maximum is found have different values in our four models. For the similar models M1 and M2 (top plots of Fig. 5), we obtain $N_c(max) = 9$ and $N_c(max) = 10$ at $n_{cut} = 5{\times}10^4$ cm^{-3} and $n_{cut} = 4{\times}10^4$ cm^{-3}, respectively. For model M3, we obtain $N_c(max) = 3$ at the cutoff densities $n_{cut} = 4{\times}10^4$ and $5{\times}10^4$ cm^{-3}. Finally, for model M4 we find $N_c(max) = 12$ at $n_{cut} = 5{\times}10^4$ cm^{-3}.

From the comparison between Figs. 6 (M1) and 7 (M2), we see that no important differences in the fragmentation process are produced by changing the amplitude A of the initial density stratification of the neutral clump. On the other hand, Figs. 8 and 9 (models M3 and M4, respectively) show that an increase of the characteristic wavelength λ leads to an important difference in the number of condensations N_c at different cutoff densities n_{cut}. In addition, from a comparison between Figs. 6 (M1) and 9 (M4) we see that the variation of the orientation angle θ also produces important changes in the fragmenta-

tion of the neutral clump. In particular, the model with $\theta = 0$ gives the maximum number of condensations obtained from our models.

4. CONCLUSIONS

In the numerical simulations of the interaction of an impinging wind+ionizing photon flux with a neutral clump developed by Raga et al. (2005), it was shown that the presence of an intense ionizing photon flux reduces the fragmentation of the clump. In order to investigate if the ionizing radiation is able to fragment a nonuniform neutral clump, we have computed 3D numerical simulations of photoevaporating clumps with strong density inhomogeneities.

In our simulations, we have studied four different models (M1–M4) with the amplitude A, the characteristic wavelength λ, and the orientation θ of the sinusoidal density stratification with respect to the plane-parallel ionizing photon flux; (Eq. [1]) as the free parameters. As the clump is photoevaporated, we see in our simulations (for all models) that an irregular ionization front is formed because regions with different densities at different positions within the clump photoevaporate at different rates. Our simulations also show that the nonuniform clump moves (by the rocket effect) along the x-axis to the right of the central position of the initial clump and forms an elongated, high density, structure before the neutral material is completely photoevaporated.

We also find from our simulations that the impinging ionizing photon flux produces fragmentation (at intermediate evolutionary states) in the neutral clump. We study this fragmentation by counting the number of condensations at different cutoff densities. We obtain from this study that for low enough cutoff densities the clump is seen as a single condensation, for cutoff densities higher than the maximum density found in each simulation no clumps are detected, and for intermediate cutoff densities the number of condensations increases with the cutoff density until a maximum is reached.

From our different models (M1–M4), we find that no important differences in the fragmentation process are produced by changing the amplitude of the initial density variability of the neutral clump, but the changes of the characteristic wavelength and the rotation of the density stratification have important effects in the fragmentation of the clump. We find that in models in which the density stratification is aligned with respect to the impinging ionizing radiation, the photons penetrate deeper into some regions of the neutral clump and, with an appropriate value of the amplitude and wavelength of the density variability (model M4), can produce hollows in the clump before it is completely photoevaporated. However, even for our more strongly fragmented model M4, we find that the neutral fragments are mostly connected by tongues of neutral material, and are not completely separate from each other (see Figs. 4 and 5).

Our simulations show that short-lived, high density condensations are produced in all models. However, in our four models, the neutral condensations are connected by bridges of neutral material, and are therefore not isolated from each other. The model which comes closest to producing several isolated neutral clumps (surrounded purely by ionized material) is model M4, which has a sinusoidal density variability aligned with the direction of the impinging photon field, with an amplitude of 90% and a spatial wavelength of one half of the clump radius (see Eq. 1). From this we conclude that in order to produce isolated neutral fragments, it is necessary to have an initial density perturbation with an amplitude of at least 90%, with a spatial wavelength comparable to the initial clump radius, and with coherent structures aligned with the direction of the impinging photon field.

In the present paper we have extended the work of Raga et al. (2005) to the case of clumps with strong initial density fluctuations. We find that the interaction of such a clump with an impinging, plane-parallel ionizing photon flux only leads to the production of more or less separate neutral clumps if the initial fluctuations are strong, and if the structures are aligned with the direction of the impinging photon flux. Therefore, the fragmentation of a photoevaporated clump clearly implies the presence of strong, coherent density inhomogeneities in the initial clump structure.

This work was supported by the CONACyT grants 41320-F and 43103-F, and the DGAPA (UNAM) grants IN 112602 and IN 111803. We thank Prof. J. Dyson for his helpful comments and suggestions.

REFERENCES

Bally, J., O'Dell, C. R., & McCaughrean, M. J. 2000, AJ, 119, 2919

Bertoldi, F. 1989, ApJ, 346, 735

Bertoldi, F., & McKee, C. F. 1990, ApJ, 354, 529

Cantó, J., Raga, A. C., Steffen, W., & Shapiro, P. 1998, ApJ, 502, 695

Dyson, J. E. 1968, Ap&SS, 1, 388

Henney, W., & Arthur, S. J. 1998, AJ, 116, 322

Henney, W., Raga, A. C., Lizano, S., & Curiel, S. 1996, ApJ, 465, 216
Lefloch, B., & Lazareff, B. 1994, A&A, 289, 559
Mellema, G., et al. 1998, A&A, 331, 335
O'Dell, C. R., Wen, Z., & Hu, X. 1993, ApJ, 410, 696
Oort, J. H., & Spitzer, L. Jr. 1955, ApJ, 121, 60
Pastor, J., Cantó, J., & Rodríguez, L. F. 1991, A&A, 246, 551
Pavlakis, K. G., Williams, R. J. R., Dyson, J. E., Falle, S. A. E. G., & Hartquist, T. W. 2001, A&A, 369, 263
Raga, A. C., Navarro-González, R., & Villagrán-Muniz, M. 2000, RevMexAA, 36, 67
Raga, A. C., & Reipurth, B. 2004, RevMexAA, 40, 15
Raga, A. C., Steffen, W., & González, R. F. 2005, RevMexAA, 41, 45
Reipurth, B. 1983, A&A, 117, 183

Ricardo F. González: Centro de Radioastronomía y Astrofísica, UNAM, Apdo. Postal 3-72 (Xangari), 58089 Morelia, Michoacán, México (ricardo@astrosmo.unam.mx).
Alejandro C. Raga: Instituto de Ciencias Nucleares, UNAM, Apdo. Postal 70-543, 04510 México, D. F., México (raga@nucleares.unam.mx).
Wolfgan Steffen: Instituto de Astronomía, UNAM, Apdo. Postal 877, 22860 Ensenada, B. C., México (wsteffen@astrosen.unam.mx).